URSI - RCRS 2022, IIT (Indore), India, 1 - 4 December, 2022

Lightning to rainfall ratio: a global perspective

R. Chakraborty* (1), P. S. Menghal (2) and A. Chakraborty (1)
(1) Divecha Centre for Climate Change, IISC, Bangalore, India,
(2) Department of Earth And Climate Sciences, IISER Tirupati, Andhra Pradesh, India,

Abstract

The present study has attempted to explain the spatiotemporal distributions of lightning to rainfall ratios. A detailed analysis revealed that the lightning to rainfall ratio is prominent near the equator, followed by the horse latitudes experiencing cooler and arid conditions. However, longitudinally, these ratios peak only around large landmasses in contrast to rainfall. Further, the equatorial African regions experience an arid climate with unprecedented lightning due to orographic convection leading to the maximum lightning to rainfall ratio values. The thermodynamic properties depict a single but gradual peak slightly north of the equator. At the same time, the longitudinal variation reveals consistently higher values of instability and clouds over land due to its lower heat capacity. Further, these observations are also supported by the seasonal variations except for the presence of prominent seasonality across the subtropical land regions.

1. Introduction

The tropical regions commonly experience frequent severe thunderstorms [1-5]. But among all among all its byproducts, rainfall and lightning pose the greatest socio-economic hazard in daily life. Speaking of these factors, rainfall and lightning flashes are highly correlated in the tropics, where intense convection gives rise to extreme events throughout the year. Hence, a series of studies have been attempted in the past decades to unravel the spatiotemporal distribution of rainfall. Some of these studies have pointed out that the tropics experience a permanent zonal rainfall band called the ITCZ (inter tropical convergence zone), which is centered slightly north of the equator due to excessive land heating [6]. On the other hand, many other researchers have investigated the spatial distribution and long-term trends of lightning [7-9]. Notably, some other recent researches have depicted that mountainous regions typically experience orographic lifting, leading to rainfall and lightning [10].

Since lightning and rainfall happen to be associated by-products of thunderstorms occurring over the tropics, there was also a need to quantify their relative contribution with respect to thunderstorm severity in various regions of the globe. Accordingly, a series of researches have attempted to investigate the distribution of such parameters from multiple perspectives. A recent study over the African region highlighted substantially alleviated lightning to rainfall ratios in the drier desert regions above 20°N in the tropics [11]. A similar study also upheld this hypothesis over the arid Australian regions but remarked that the contrast in such ratios becomes more prominent during the local summer season [12]. Likewise, a recent study also depicted that land regions are more sensitive to lightning than rainfall globally, especially in locations towards the edges of the tropics [13].

But despite multiple attempts to decipher these factors, there is still a dearth of holistic and in-depth approaches to investigate the lightning to rainfall balance globally as well as for different seasons. In addition, there is also a need to understand the underlying mechanisms for the observations reported earlier, enabling us to understand the interactions between rainfall and lightning to a much better extent. Hence the present study attempts to investigate the spatiotemporal distributions of lightning, precipitation, and their ratios globally, along with their potential controlling factors, namely: instability, clouds and moisture content, both annually and seasonally.

2. Dataset

In this study, lightning frequency datasets are utilized from Lightning Image Sensor (LIS) observations onboard the Tropical Rain Measurement Mission (TRMM) satellite, while the gridded monthly average rainfall estimates have been taken from the TRMM 3B42 archives during the years 1998-2014 at a uniform resolution of 0.25° X 0.25° globally. Secondly, datasets from the fifth generation European Centre for Medium-Range Weather Forecasts (ECMWF) reanalysis, ERA5 datasets are used at 0.25° resolution to unravel the implications holding lightning and rainfall with other metrological factors.

3. Results and Discussion

3.1. Spatio-temporal variation of lightning rainfall ratio

Firstly, we look at how lightning is distributed from 90°N to 90°S. On an annual average, we know that solar radiation is highest at the equator and uniformly decreases as one goes on either side of the 0° latitude. However, lightning flashes peak across ±5°N with a slight deviation of the peak towards the North (Figure 1). Notably, this deviation is also seen in ITCZ owing to a larger percentage of the landmass in the Northern Hemisphere than the Southern counterpart. Beyond 5° in both hemispheres, lightning flashes reduce drastically till around 30°N, S, where the values plateau for a brief extent and then start decreasing again till the poles. Even this plateau of

lightning flash values is higher in the North than in the south. This could be due to higher heating of the northern hemisphere as well as the presence of the Himalayas, which assists more flashes via orographic convection.

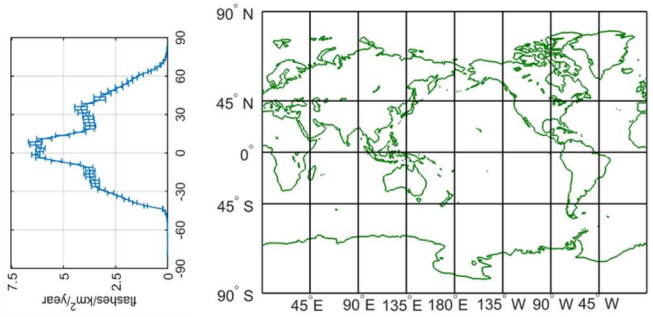

Figure 1. Latitudinal distribution of lightning frequency and world map for reference

Lightning, rainfall, and thunderstorms are predominantly convective phenomena. Thus, we see a higher frequency of the same in the tropics, the region most heated at the surface. We thus, limit our study area to the tropical region to closely analyze the phenomenon and its variability. Herein, rainfall and lightning flash rate values are normalized to represent values between -1 to 3 and -2 to 2, respectively, to make them more comparable. Subsequently, the distribution of these parameters is depicted in Figure 2. Rainfall has a peak slightly towards the North of the Equator but then it decreases drastically as we move away from it. Lightning flashes, however, have a symmetrical distribution across the equator, with peak values near the equator and a slight and steady decrease beyond the peaks.

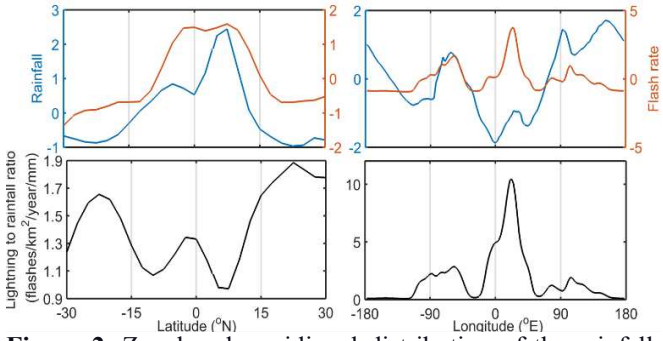

Figure 2. Zonal and meridional distribution of the rainfall, lightning, and lightning to rainfall ratio

Consequently, the lightning to rainfall ratio depicts a smaller maximum at the equator since rainfall distribution is biased towards the North of 0° latitude. Next, a minimum is found on either side of this equatorial maximum, indicating the latitude where a maximum rainfall is present. Beyond these however, lightning efficiency increases owing to the disproportionate decrease in rainfall and lightning flash rates.

The key to observing the longitudinal distribution of rainfall, lightning flash rates and lightning efficiency would arise from their geospatial characteristics across the tropics. A corresponding figure on the world map is also hence provided for comparison. Rainfall shows an erratic pattern, but its distribution fairly agrees with the presence of the oceans, deserts and ENSO regions. Lightning, however, is straightforward, peaking in the regions of substantial landmass. Hence, lightning efficiency shows higher values over the landmasses but with varying magnitudes. While South America (45°-90°W) and SE Asia (90°-120°E) experience significant amounts of lightning, rainfall is also present. However, across N and S Africa (0°-30°E), we experience arid regions with unprecedented amounts of lightning. Hence, we observe the peak lightning to rainfall ratios across this longitude band.

Next, the seasonal analysis of the distribution is attempted to uncover the major atmospheric variables present during various phases of the solar cycle, which is the main driver of climate. Subsequently, the distributions are taken for three different parts of the year, depicting North Hemisphere Summer (April, May, June, July), North Hemisphere Winter (October, November, December, January) and Equinox (February, March, August, September). Then we plot the variations for all these parameters in Figure 3. The summers are associated with higher surface heating; thus, we note higher lightning flash rates and rainfall in their respective hemispheres during this period. Notably, these summer peaks are confined within 5°S and 10°N. However, we find an extreme minimum in rainfall and lightning flash rates in winter seasons. Equinoctial months represent the averaged value of the opposite seasons, thereby depicting a symmetric variation. Consequently, the lightning to rainfall ratio peaks once at the equator and then at the edge of the tropical regions. This suggests that lightning flashes persist further than rainfall as we move away from the equator especially in winter when rainfall is scarce. But notably, the extreme maximum values are observed at 10°-15° N due to the absence of rain even as few lightning flashes occur there.

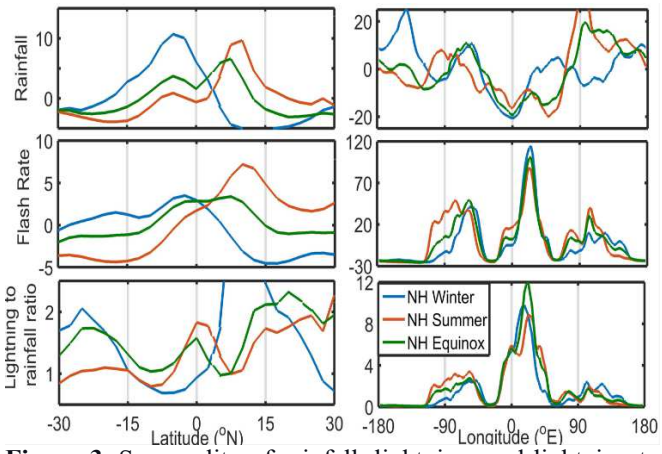

Figure 3. Seasonality of rainfall, lightning, and lightning to rainfall ratio

As mentioned before, rainfall is distributed erratically across the longitudes, with local maxima around 150°E, where rainfall is high in NH winter, and this is again due to EL-Nina and La-Nina conditions that time of the year. Next, around 90°E, in NH Summer, maximum rainfall is seen, which can be attributed to monsoons and local cyclonic activity. A minimum is noted along the prime meridian due to extremely dry regions such as the Sahara and Namib desert along this longitude. Next, as expected, lightning flash rates peak extensively over the landmasses with the highest values in

Africa as a combination of multiple factors such as orography and differential land sea heating. Lightning efficiency follows the same distribution as lightning flash rates. However, its values over the African continent are significantly higher than that over the Americas and SE Asia. This could be due to the lower rainfall average across Africa, as opposed to the Americas and SE Asia, where heavy rainfall occurs. The minima in flash rates and lightning ratio is seen in regions dominated by the seas, namely the Atlantic, Pacific, and Indian oceans, as they do not experience sufficient atmospheric instability for intense lightning occurrences.

3.2. Mechanisms explaining the spatiotemporal distribution of lightning to rainfall ratio

We now try to understand the probable causes leading to these distributions depicted above by considering the thermodynamic properties of the atmosphere. This attempt can be justified because lightning originates from the collisions of ice and graupel particles within the cloud. Since the atmosphere cools with altitude, such icy particles form in the atmosphere only when the clouds are sufficiently high enough to allow the water vapor to freeze either homogeneously or heterogeneously. Convective Available Potential Energy (CAPE) corresponds to this potential energy required by the vapor to form such hydrometers and thus forms the main driving factor behind lightning genesis.

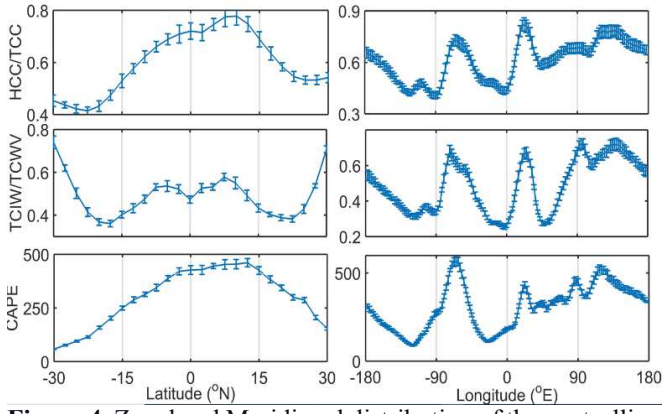

Figure 4. Zonal and Meridional distribution of the controlling factors: HCC/TCC, TCIW/TCWV and CAPE.

Next, it is known that a cloud extending beyond 7 Kilometers is cold enough to freeze all the water vapor present. Hence, to study the distribution of clouds that can host particles conducive for lightning genesis, the ratio of high cloud cover (clouds with tops beyond 7 Kilometers) to total cloud cover is observed spatially along the latitudes and longitudes in Figure 4. Across the Latitudes, a peak North of the equator, along with a steady decrease towards the edges of the tropics. In contrast, we observe the peaks coinciding with the distribution of landmasses again across all longitudes. However, here we also see a high peak in values along SE Asia and Australia which can be due to frequent and severe cyclonic storms there.

Next, the ratio of total cloud ice water to the total cloud water vapor (TCIW/TCWV) is observed as it depicts the number of ice particles in the moist atmosphere that could generate lightning. Typically, the water vapor content is ~1000 times more than the ice water. Thus, for normalization, we multiply the ratio by 1000. Across the latitudes, we observe a symmetric distribution about the equator. Further, some small local peaks emerge on both sides of the equator, after which it again increases near the edge of the tropics, despite a decrease in High cloud cover in the corresponding latitude. This could be due to local convection and a reduction in the height at which freezing occurs since incoming solar radiation decreases as we move away from the equator. In addition, the geolocation of large landmasses and oceans explain the increased and decreased distribution of TCIW/TCWV, respectively. Finally, coming to CAPE, we find that it is higher over the land than the sea regions due to its lower heat capacity. Here it may be noted that the tropical zones in the northern hemisphere have a larger percentage of landmass than the southern counterpart, and as expected, CAPE follows this distribution as well. In the longitudes, we observe that HCC/TCC and CAPE follow a near identical distribution, albeit with minor differences, since CAPE is strictly a local phenomenon, while the extent of cloudiness may also et influenced by mesoscale and synoptic scale interactions as well. Apart from that, considerably lower values of all the above variables are seen over longitudes covering the calm seas of West Pacific, Atlantic and the Indian Ocean.

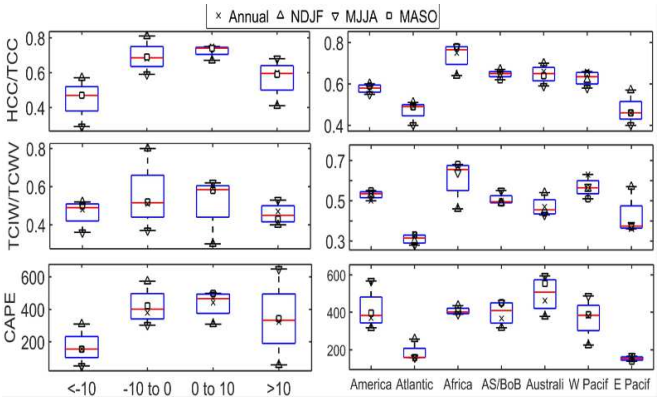

Figure 5. Seasonality of HCC/TCC, TCIW/TCWV and CAPE with respect to latitude and longitude.

Finally, we investigate the seasonal variations of the atmospheric parameters in Figure 5 to see whether they conform with the lightning to rainfall ratio distributions. For simplicity, we divide the latitudinal span into four different parts (< -10°N, -10°N - 0°, 0°- 10°N and <10°N) while the longitudes are sectored into the dominant landmass and oceanic regions namely: Americas, Atlantic Ocean, Africa, Asia-Bay of Bengal, Australia, West Pacific and East Pacific.

Since areas near the equator receive the highest amount of solar radiation, we observe that the values of all parameters were higher in regions near the equator than those noted beyond 10° in each hemisphere. Next, higher variability in these values is seen in the regions afar the equator due to significant variability in incoming solar radiation across different seasons. Furthermore, we see that all these parameters depict their primary peaks in opposing seasons in each hemisphere. For example, HCC, TCIW and CAPE are highest in the local summers and lowest during winters in their respective hemispheres. Longitudinally, the highest values are observed in the largest landmasses, while lower magnitudes and variability are seen in the oceanic regions.

Next, HCC/TCC and TCIW/TCWV are prominently higher in Africa due to various factors otherwise absent in the Americas and Australia. These include convergence from either side of the continent due to land-sea differential heating and enhanced orography. CAPE, however, is comparable between Africa and the other longitude bands due to dearth of moisture in certain regions of Africa, which also otherwise plays a major role in increasing CAPE like land heating, unlike the longitudes involving the Americas, Australia, and SE Asia.

4. Conclusions

The present study attempts to decipher the global spatiotemporal distributions of lightning to rainfall ratios. A detailed statistical analysis revealed that the lightning to rainfall ratio is prominent near the hot and moist equator, followed by the horse latitudes experiencing cooler and arid conditions. However, longitudinally, these ratios peak only around the large landmasses unlike rainfall. Further, the equatorial African regions experience an arid climate with unprecedented lightning due to orographic convection leading to maximum lightning to rainfall ratio values. Subsequently, the thermodynamic properties depicted a single but gradual peak slightly north of the equator thereby supporting the geospatial distributions of the lightning to rainfall ratios. Further, the longitudinal variation reveals consistently higher values of instability and clouds over the landmasses due to their lower heat capacity. Finally, the seasonal variations also support these observations, except for the presence of prominent seasonality across the subtropical land regions in both hemispheres compared to the equatorial areas.

5. Acknowledgements

R. Chakraborty acknowledges the financial support provided by INSPIRE faculty research grant from DST (DST/INSPIRE/04/2019/002096) for this research work.

References

[1] R. Chakraborty, S. Das, S. Jana, A. Maitra, "Nowcasting rain events using multi-frequency radiometric observations", *Journal of Hydrology,* **513,** 2014, 467 – 474, DOI: 10.1016/j.jhydrol.2014.03.066

[2] A. Maitra, R. Chakraborty, "Prediction of Rain Occurrence and Accumulation using Multifrequency Radiometric Observations", *IEEE Transactions Geoscience and Remote Sensing*, **56(5)**, 2018, DOI: https://doi.org/10.1109/TGRS.2017.2783848

[3] A. Maitra, G. Rakshit, S. Jana, R. Chakraborty, "Effect of Boundary Layer Dynamics on Profiles of Rain Drop Size Distribution During Convective Rain," *IEEE Geoscience and Remote Sensing Letters*, **16(7)**, 2019, 1007-1011, Doi: https://doi.org/10.1109/LGRS.2019.2891906

[4] R. Chakraborty, B.K. Guha, S. Talukdar, M. Venkat Ratnam, A. Maitra, "Growth in mid-monsoon dry phases over the Indian region: prevailing influence of anthropogenic aerosols", *Atmospheric Chemistry and Physics*, **19(19)**, 2019, pp. 12325-12341, DOI: https://doi.org/10.5194/acp-19-12325-2019

[5] R. Chakraborty, S. Das, A. Maitra, "Prediction of convective events using multi-frequency radiometric observations at Kolkata", *Atmospheric Research,* **169(A),** 2016, 24-31 DOI: https://doi.org/10.1016/j.atmosres.2015.09.024

[6] Philander, S. G. H., D. Gu, G. Lambert, T. Li, D. Halpern, N-C. Lau, and R. C. Pacanowski. "Why the ITCZ Is Mostly North of the Equator". *Journal of Climate* **9(12)**, 1996, 2958-2972. https://doi.org/10.1175/1520-0442(1996)009

[7] Y.A. Liou S.K. Kar, "Study of cloud-to-ground lightning and precipitation their seasonal geographical characteristics over Taiwan", *Atmospheric Research*, **95**, 2014, 115–122 Doi: https://doi.org/10.1016/j.atmosres.2009.08.016

[8] R. Chakraborty, G. Basha and M. Venkat Ratnam, "Long-term trends of instability associated parameters over Indian region obtained using a radiosonde network", *Atmospheric Chemistry and Physics,* **19(6),** 2019, 3687–3705. https://doi.org/10.5194/acp-19-3687-2019

[9] R. Chakraborty, A. Chakraborty, G. Basha, M. Venkat Ratnam, "Lightning occurrences and intensity over the Indian region: long-term trends and future projections", *Atmospheric Chemistry and Physics,***21,** 2021, pp. 11161-11177, https://doi.org/10.5194/acp-21-11161-2021

[10] V. Bourscheidt, O.P. Junior, K.P. Naccarato and I.R.C.A. Pinto, "The influence of topography on the cloud to-ground lightning density in South Brazil". *Atmospheric Research*. **91**, 2009, 508–513, https://doi.org/10.1016/j.atmosres.2008.06.010

[11] Finney, D. L., Marsham, J.H., Wilkinson, J. M., Field, P. R., Blyth, A. M., Jackson, L. S., "African lightning and its relation to rainfall and climate change in a convection-permitting model". *Geophysical Research Letters*, **47**, 2020 e2020GL088163. https://doi.org/10.1029/2020GL088163

[12] Jayaratne, R Kuleshov, E, "Geographical and seasonal characteristics of the relationship between lightning ground flash density and rainfall within the continent of Australia". *Atmospheric Research* **79(1)** 2006, 1-14. https://doi.org/10.1016/j.atmosres.2005.03.004

[13] Takayabu, Y.N. "Rain-yield per flash calculated from TRMM PR and LIS data and its relationship to the contribution of tall convective rain". *Geophysical Research Letters*, **33**, 2006, https://doi.org/10.1029/2006GL02753